THE APPLICATION OF SCINTILLATION SPECTROSCOPY TO AN INVESTIGATION OF THE NEUTRON INDUCED EUROPIUM ACTIVITIES

by

HAROLD SIMS BUTLER

B. A., Phillips University, 1953

A THESIS

submitted in partial fulfillment of the

requirements for the degree

MASTER OF SCIENCE

Department of Physics

KANSAS STATE COLLEGE
OF AGRICULTURE AND APPLIED SCIENCE

1956

TABLE OF CONTENTS

PREFACE

In 1913 Niels Bohr announced his famous theory of the atom. This theoretical atom was a model which provided an explanation of spectral lines in terms of transitions in an excited atom. One consequence of the Bohr theory was the development of the concept of energy levels and energy level diagrams. This concept proved to be extremely useful and enlightening in the field of atomic spectra.

Later on as research progressed in nuclear physics, it was discovered that the excited nucleus decayed in a manner analogous to the excited atom. The analogy was so close that it was possible to apply the concept of energy level diagrams to nuclear energy levels. This application spawned a tremendous research effort by scientists all over the world to establish decay schemes for the isotopes of the various elements by experimental means.

It has been the aim of this author's research to add to the wealth of knowledge being accumulated about nuclear decay. The author hopes that it will provide some insight to a future Niels Bohr which will enable him to unravel the secrets of the nucleus.

INTRODUCTION

A radionuclide may decay by means of a number of different processes. Of these various processes three are closely related—negatron emission, positron emission, and K-capture. The general term "beta-decay" is given to all three. Their similiarity lies in the fact that in each process the total number of nucleons (protons and neutrons) in the nucleus remains unchanged.

In the case of negatron emission, better known as β^- decay, one of the neutrons in the nucleus is transformed into a proton with the accompanying emission of an electron, β^-, and a neutrino, ν. An example of this transformation is

$$_{63}Eu^{152} \longrightarrow {}_{64}Gd^{152} + \beta^- + \nu$$

In positron emission, commonly denoted as β^+ decay, a proton in the nucleus transforms into a neutron by emitting a positron, β^+, and a neutrino. An example is

$$_{63}Eu^{150} \longrightarrow {}_{62}Sm^{150} + \beta^+ + \nu$$

The term K-capture is given to that process in which an orbital electron (most probably from the K orbit) is absorbed into the nucleus, resulting in the transformation of a proton to a neutron. The K-capture process is exemplified by

$$_{63}Eu^{152} + e^- \longrightarrow {}_{62}Sm^{152} + \nu$$

The product nucleus in each of the above three processes is not generally in the ground state; rather it usually is in some excited state. Subsequently,

the excited nucleus gets rid of its excess energy by gamma emission. This process is illustrated by

$$_{62}Sm^{152*} \longrightarrow {}_{62}Sm^{152} + \gamma$$

The excited nucleus may also decay by the process of internal conversion in which an orbital electron perturbs the excited nucleus and induces a transition to a lower energy state. The transition energy is transferred to the electron which is forced from its orbit and appears outside the atom with a kinetic energy, E_e, given by

$$E_e = E_\gamma - E_b$$

where E_b is the binding energy of the electron in its orbit and E_γ is the energy of the gamma ray.

In addition to gamma radiation, accompanying x-rays characteristic of the element undergoing decay are emitted in the case of K-capture and internal conversion.

If, then, one investigates the gamma and x-radiation and the energetic electrons accompanying these three processes, it is possible to obtain useful information concerning the nucleus. One end product of such investigations is the establishment of a decay scheme which is a pictorial representation of the various modes of decay by which the parent nucleus transforms to the ground state product nucleus. Customarily, both beta and gamma transitions are pictured on the diagram. Plate IX is an example of a typical decay scheme. One of the purposes of this thesis is to propose decay schemes for $_{62}Sm^{152}$, $_{64}Gd^{152}$, and $_{64}Gd^{154}$.

The experimental methods used to investigate the gamma radiation accompanying beta decay center around two general types of instruments. The first

is the 180° deflection beta-ray spectrograph which has been discussed in detail by Mellor (13). The second instrument is the scintillation spectrometer and it is this instrument with which this thesis will be primarily concerned.

INSTRUMENTATION

The bulk of the experimental data appearing in this thesis was obtained through the use of two scintillation spectrometers and a coincidence counter. Plate I is a photograph of the assembled equipment. Each spectrometer consists of a crystal detector, a pulse-height analyzer, a high voltage power supply and a scaler. Plate II shows a block diagram of the scintillation spectrometer.

This section is devoted to outlining the operation of these instruments. It is not the purpose of this section to present a detailed discussion of the instruments but rather to describe only the pertinent features of their operation that influence the form in which data is obtained from them. A thorough technical discussion of the operating principles of these instruments, including circuit diagrams, may be found in the manufacturer's operation manual (8).

The Crystal Detector

The crystal detector[1] of the scintillation spectrometer consists of a thallium-activated sodium iodide crystal[2], a photomultiplier tube and a

---

[1] Model 43A Scintillation Counter, Radiation Instrument Development Company.

[2] Sintilon Brand Mounted Sodium Iodide (Tl) Crystal, National Radiac, Inc.

EXPLANATION OF PLATE I

Photograph of the assembled coincidence spectrometer used in this investigation.

A.....Coincidence Counter
B1, B2.....Scalers
C1, C2.....Pulse Height Analyzers
D1, D2.....High Voltage Power Supplies
E1, E2.....Crystal Detectors

A block diagram of the interconnections among the instruments is shown on Plate V.

PLATE I

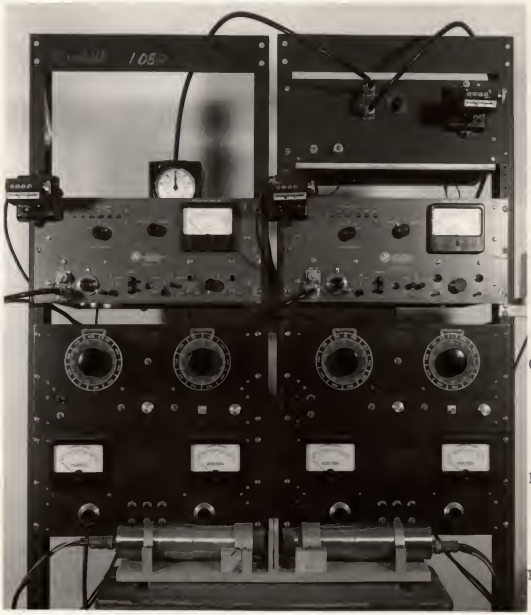

EXPLANATION OF PLATE II

Block diagram of a scintillation spectrometer showing the history of three different gamma rays.

PLATE II

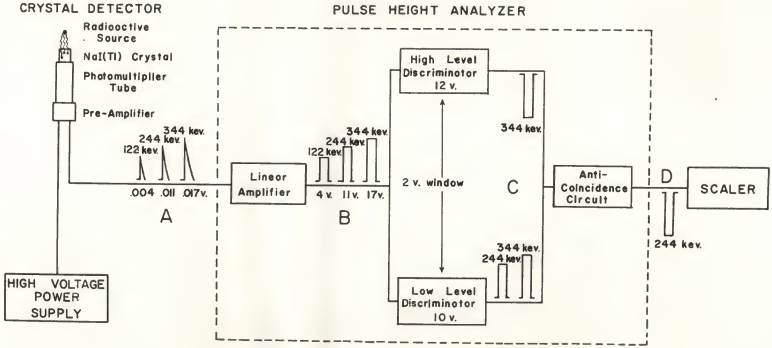
CRYSTAL DETECTOR
PULSE HEIGHT ANALYZER
Radioactive Source
NaI(Tl) Crystal
Photomultiplier Tube
Pre-Amplifier
122 kev.
244 kev.
344 kev.
.004 .011 .017v.
A
Linear Amplifier
4 v. 11v. 17v.
B
High Level Discriminator 12 v.
Low Level Discriminator 10 v.
2 v. window
C
Anti-Coincidence Circuit
D
SCALER
HIGH VOLTAGE POWER SUPPLY

preamplifier circuit. When a gamma ray of any given energy strikes and is absorbed[1] by the crystal, a spectrum of photons is produced. The crystal is mounted in such a manner that a portion of the scintillations produced in the crystal is detected by the light sensitive anode of the photomultiplier tube. The signal produced at the output of the photomultiplier tube has the form of a voltage pulse which is proportional to the energy of the gamma ray initially incident upon the crystal. This output pulse then passes to a linear preamplifier. Thus the output pulse from the crystal detector unit is proportional to the energy of the initial gamma ray.

The Pulse Height Analyzer[2]

The voltage pulses forming the output of the crystal detector are fed to the pulse-height analyzer which consists of a linear amplifier, a low level discriminator, a high level discriminator, and an anti-coincidence circuit.

The linear amplifier utilizes two feedback loops and has an overall maximum gain of one thousand. The maximum gain may be reduced by factors of 1/2, 1/4, 1/8, and 1/16. All pulses entering this unit are amplified and passed simultaneously to both discriminator circuits.

The low level discriminator circuit (commonly called the channel level) is designed to pass only those voltage pulses whose magnitude is greater than a pre-selected voltage, V(low). Any pulse meeting this requirement

---

[1] Not every gamma ray impinging upon the crystal is absorbed. The reason for this fact and the consequences of it are discussed in the section on The Collection and Treatment of Experimental Data.

[2] Model 115 Single Channel Pulse Height Analyzer, Radiation Instrument Development Laboratory.

triggers an equal pulse to the anti coincidence circuit. The arbitrary voltage, V(low), is set on a ten-turn potentiometer and can be varied from 0-100 volts.

The high level discriminator can be varied by a ten-turn potentiometer over a range from 0-10 volts. The voltage set on this potentiometer is commonly referred to as the window voltage or the window width. The window voltage is always referenced to the low level discriminator voltage, in other words, is added to it--V(low) + V(window). But at the same time, the window width is independent of the voltage which is set on the channel level. For example, a two volt window width remains two volts whether the channel level is set at 5 or 75 volts. Any voltage pulse entering the high level discriminator circuit and having a magnitude greater than the sum--V(low) + V(window)--is passed on as a negative but equal pulse.

Both discriminator circuit outputs are fed simultaneously to the anti-coincidence or gate circuit. This circuit monitors the incoming pulses, screens out all coincident pulses and passes the rest to the scaler for counting.

As a result of this arrangement of electronic circuits, the pulse height analyzer permits only those pulses to be counted which have a voltage height greater in magnitude than V(low) but less than V(low) + V(window). But since the height of any pulse is proportional to the energy of the initial gamma ray giving rise to the pulse, the pulse height analyzer allows the counting of only those gamma rays whose energies lie between E and E + dE.

The overall operation of the pulse height analyzer can be clarified by an example. Plate II gives the history of three non-coincident gamma rays having energies of 122, 244, and 344 kilovolts (kev) which strike the sodium iodide crystal. They are converted in the crystal - photomultiplier - pre-

amplifier combination to three strictly proportional voltage pulses of .004, .011 and .017 volts respectively. These pulses are labled (A) in Plate II. The linear amplifier, normally operated at its maximum gain of 1000, then increases the heights of these pulses to 4, 11, and 17 volts, as shown at point (B). For the sake of illustration, suppose that the channel level (low level discriminator) is set at 10 volts. In this case the 4 volt pulse (122 kev gamma ray) will be rejected, whereas the 11 and 17 volt pulses will trigger a pulse to the anti-coincidence circuit. Suppose further that the high level discriminator is set at 2 volts, thus giving a total—V(low) V(window)—of 12 volts. Then only the 17 volt pulse (344 kev gamma ray) will trigger a pulse to the gate circuit. Plate II, point (C) illustrates this situation. This pulse, being equal but negative to the corresponding 17 volt pulse triggered by the low level discriminator, will cancel it out when they arrive in the anti-coincidence circuit. However the 11 volt pulse, corresponding to the 244 kev gamma ray, will not be cancelled, but rather will be counted by the scaler. The result is shown in Plate II, point (D).

Had the channel level been set at three volts with the same two volt window width, the 122 kev gamma ray would have been counted. Likewise, with a channel level setting of 16 volts and a two volt window the pulse height analyzer would have selected the 344 kev gamma ray.

From this example it can be seen that by setting the appropriate channel level and window width on the pulse height analyzer, it is possible to select gamma rays of any chosen energy.[1] Since the channel level can be varied continuously from 0-100 volts, it is possible to investigate the whole gamma ray energy spectrum up to any desired energy. The operational procedure

---

[1]This statement will be qualified in the following two paragraphs.

consists of setting the channel level, obtaining the gamma ray counting rate at this level, then repeating the process at different channel levels until the spectrum is surveyed as far as desired. A record is kept of the counting rate obtained at each channel level setting.

Plate III illustrates the gamma ray line shape produced by the spectrometer. The line shape of an abundant 344 kev gamma transition is plotted for several different window widths. The line width at half peak intensity increases only slightly with increasing window width. This suggests that the curves plotted represent very nearly the natural line shape to be expected from the instrument. The line shape is determined by intrisic properties of the scintillation crystal.

Plate III also gives a measure of the resolution to be expected from the spectrometer. It is known from beta-ray spectrograph data that a second weaker gamma ray of energy 335 kev lies hidden in the 344 kev line. This accounts for the splitting at the peak of several of the curves. The point to be made is that in general it is impossible to single out any one gamma ray. At best only a range of energies can be counted for any given setting of the channel level and window width.

The High Voltage Power Supply[1]

The purpose of the regulated high voltage power supply is to produce the accelerating potential for the photomultiplier tube. The magnitude of this accelerating potential determines the proportionality constant between the gamma ray energy and the voltage of the output pulse from the preamplifier.

---

[1]Model 80 Regulated Dual Precision High Voltage Supply, Radiation Instrument Development Laboratory.

EXPLANATION OF PLATE III

Line shape resulting from a 344 kev gamma ray plotted for several different window widths.

PLATE III

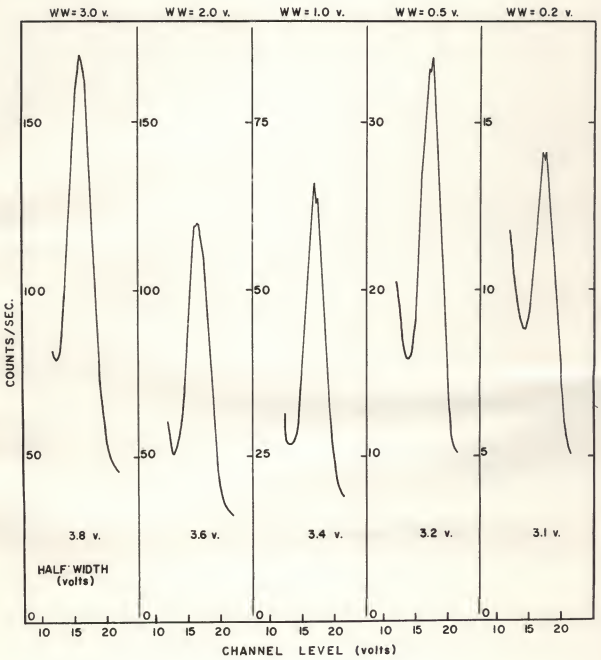
WW = 3.0 v.
WW = 2.0 v.
WW = 1.0 v.
WW = 0.5 v.
WW = 0.2 v.
COUNTS/SEC.
150
100
50
150
100
50
75
50
25
30
20
10
15
10
5
3.8 v.
3.6 v.
3.4 v.
3.2 v.
3.1 v.
HALF WIDTH (volts)
0
10 15 20
CHANNEL LEVEL (volts)

Since the high voltage is continuously variable from 500-1500 volts it is possible to vary the constant of proportionality over a wide range. This makes it possible to expand the spectrum for resolution or compress it for definition. Although the magnitude of the high voltage can be varied, it is fixed throughout any one run and held constant by an automatic built-in regulating circuit. Plate IV shows the relation between the high voltage and the channel level voltage which caused a 344 kev gamma ray to peak in.

The Scalers[1] and Coincidence Circuit

Scalers were used in this investigation to count the pulses from the output of the pulse height analyzer. A discussion of the scaling circuit utilized as the basic component of these instruments can be found in any one of several texts on nuclear physics, for instance Halliday (6), p.97.

The coincidence spectrometer described below employs a coincidence circuit which is a standard Rossi-type circuit (6), p. 203. It has a resolving time of one microsecond. The coincidences are recorded by a mechanical ratchet-type counter.

The Coincidence Spectrometer

The coincidence circuit combined with two scintillation spectrometers constitutes a coincidence spectrometer. Plate V shows a block diagram of the interconnections while Plate I is a photograph of the actual equipment. This type of spectrometer is utilized in the following manner: The channel level of spectrometer one is adjusted to select as closely as possible a certain gamma ray. The output from this instrument is fed simultaneously

---

[1] Model 162 Scaling Unit, Nuclear Instrument and Chemical Corp.

EXPLANATION OF PLATE IV

Effect of high voltage on the location and shape of a line arising from a 344 kev gamma transition.

PLATE IV

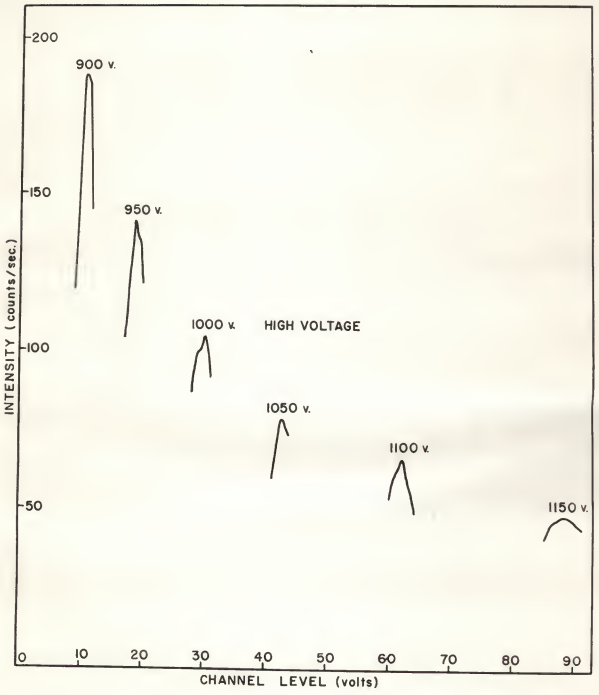
200
150
100
50
INTENSITY (counts/sec.)
900 v.
950 v.
1000 v.
HIGH VOLTAGE
1050 v.
1100 v.
1150 v.
0
10
20
30
40
50
60
70
80
90
CHANNEL LEVEL (volts)

EXPLANATION OF PLATE V

Block diagram of the coincidence spectrometer used in this investigation.

The components B1, C1, D1, and E1 taken together constitute a scintillation spectrometer, as do B2, C2, D2, and E2. When the output from each spectrometer is fed to the dual input coincidence counter, the resultant assembly constitutes a coincidence spectrometer.

PLATE V

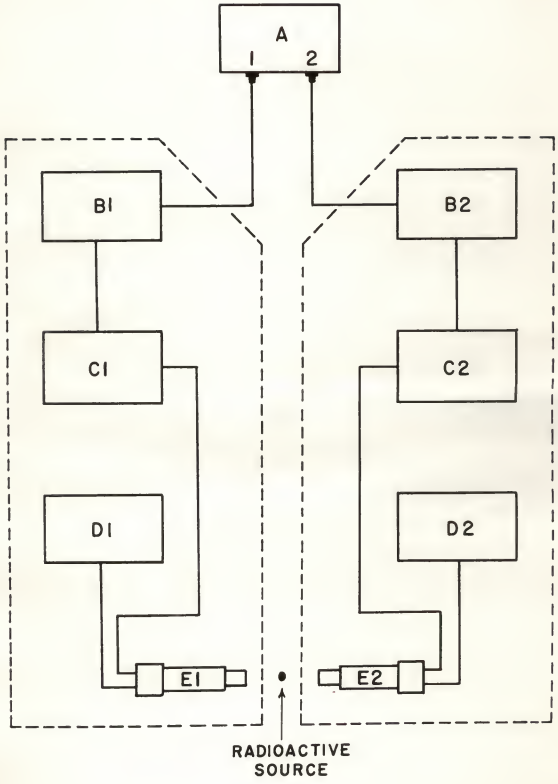

to scaler one and to input channel one of the coincidence circuit. The output of spectrometer two is fed both to scaler two and to input two of the coincidence circuit. Spectrometer two is then used to scan in incremental steps the region of the gamma spectrum under investigation. A record is kept of the count rates from scalers one and two and the coincidence circuit. In this way it is possible to determine if any gamma ray tuned in on spectrometer two is in coincidence with the gamma ray set on spectrometer one.

THE COLLECTION AND TREATMENT OF EXPERIMENTAL DATA

Corrections

The data recorded directly from the instruments during this investigation required special corrections. These corrections divided themselves into two groups—those connected with the gamma ray spectrum and those having to do with the coincidence spectrum. The gamma ray spectrum had to be corrected for leakage and background rates and for crystal efficiency. In treating the coincidence spectrum, account was taken of the losses due to the mechanical ratchet-type counter, the resolving time of the coincidence circuit and the crystal efficiency.

Gamma Ray Spectrum

Plate VI, Curve A presents the data representing the gamma ray spectrum as obtained directly from the scintillation spectrometers. It is a point by point plot with the count rates as ordinates and the channel level voltages as abscissas. The vertical bars through certain of the points indicate the 50 percent statistical uncertainty of the points. For the most part readings of the count rate were taken at 0.5 volt intervals over the whole 0-100 volt

range of the channel level control. With the particular high voltage setting employed, this interval corresponded closely to a gamma ray energy interval of eight kev.

After obtaining the gamma ray spectrum, the window width was closed to zero volts and the whole range of channel level voltages was again run in a point by point fashion. In theory the pulse height analyzer operated at zero window width should not have allowed any pulses to reach the scaler. However, in practice it was found that a number of counts were actually registered. The time rate of occurrence of these counts is referred to as the leakage count rate. It resulted from an overloading due to high count rates. Under the operating conditions given on Plate VI the magnitude of this erroneous count rate ranged from 30 percent of the total spectrum count rate at low energies to negligible amounts above 1000 kev, dropping off more or less exponentially for points in between.

The first correction to the gamma ray spectrum then consisted of subtracting the leakage count rate from the total spectrum count rate in a point by point manner for each channel level setting.

After the leakage spectrum was obtained, the radioactive source was moved well away from the vicinity of the crystal detector and the window width was restored to its original setting. With this arrangement the whole range of channel level settings was again scanned. The resultant spectrum, termed the background spectrum, arose from extraneous low level gamma radiations present in the laboratory. The background spectrum was also subtracted from the total spectrum in a point to point fashion. The magnitude of this correction under the stated operating conditions ranged from 4 percent at low energies to negligible amounts above 500 kev. Curve B of Plate VI gives the result of correcting the original gamma ray spectrum, Curve A, for leakage and background.

A third and final correction to the gamma ray spectrum was required because the NaI (Tl) crystals did not absorb gamma rays of various energies with equal probability. A theoretical consideration of this factor is presented in the Appendix, the result being a set of graphs, Plate XI, which give the correction to be applied to the gamma ray spectrum as a function of energy. When these corrections were applied to Curve B of Plate VI, the result was Curve C which was taken to be the final corrected gamma ray spectrum.

There is still another correction which some authors (McGowan, 12) apply to a gamma ray spectrum. It represents an attempt to correct for Compton scattering. Mention is made of this phenomenon in the Appendix. However, no attempt was made in this investigation to allow for it since collecting the data required for the correction would, in itself, be a major undertaking.

Therefore, it is recognized that Curve C is far from being absolutely correct. In fact, there is a good possibility that the intensity of the high energy peaks is too weak by a factor of two, perhaps even three. However, the corrections applied all appeared to modify the spectrum in the right direction. The important thing to keep in mind is that the gamma ray spectrum as it stands in Curve C is accurate enough for the uses to which it was put.

Coincidence Spectrum

Plate VII, Curve A presents representative data obtained by use of the coincidence spectrometer. As mentioned earlier the coincidence spectrum also had to be adjusted to take into account several factors which tended to reduce the meaningfulness of the data. In the first place, the mechanical

ratchet-type counter used to record the number of coincidences failed to record every one because the random nature of the counts resulted in small losses when coincidences occurred too close together. To get a quantitative measure of this loss, pulses from a radioactive source were fed simultaneously to a scaler and to the coincidence circuit. Both input channels of the coincidence circuit were shorted together so that each pulse recorded by the scaler would have registered a coincidence count in the absence of losses. Figure 1 is a plot of the ratio of the scaler count rate to the mechanical count rate (true/observed) versus the observed count rate. This graph furnishes the factors to correct for mechanical recorder losses. Curve B of Plate VII shows the result of applying this correction to two coincidence peaks of Curve A.

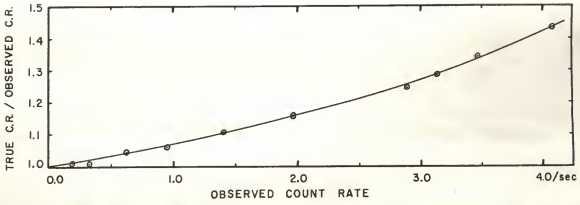

Figure 1. Curve used to correct for loss of coincidence counts due to the ratchet-type mechanical counter.

A second modification of the coincidence spectrum was necessary to correct for accidental counts. When a pulse from one spectrometer arrived at one input of the coincidence circuit, there was a small but definite probability that a pulse from the second spectrometer would arrive very

nearly simultaneously at the second input of the coincidence circuit. Although the two pulses were not truly coincident, the circuit could not resolve this fact and as a result a coincidence count was registered. The number of accidental counts accumulated in this manner depended on the resolving time of the circuit according to the equation derived by Green (4), p. 126:

$$N_{acc} = 2\tau N_1 N_2$$

where N_1 and N_2 are the count rates from the two scintillation spectrometers. The measured resolving time, τ, of the coincidence circuit used in this investigation was 1.0 microsecond and was for all practical purposes independent of gamma ray energy and count rate. Using this resolving time and the count rate from each spectrometer, the number of accidentals for each point on the coincidence spectrum was calculated. Plate VII, Curve C shows the result of applying this correction to the two low energy peaks of Curve B.

It should be noted that the corrections leading to Curves B and C were small, even though these were the most intense peaks in the spectrum. Moreover, the corrections tended to cancel each other. As a result it was unnecessary to adjust the spectrum beyond these first two peaks.

Finally, the coincidence spectrum was modified to take into account the efficiency of the crystals. The technique was the same as described earlier for the gamma ray spectrum. Application of this correction to Curve C[1] of Plate VII furnished the final corrected coincidence spectrum shown as Curve D.

---

[1]Note that there is no distinction between Curve C and Curve A beyond the first two peaks.

INVESTIGATION OF EUROPIUM ACTIVITIES

The instruments discussed in the section on Instrumentation were used to investigate gamma radiation from two even-even europium isotopes, $_{63}Eu^{152}$ and $_{63}Eu^{154}$. These isotopes were derived by pile irradiation of the pure odd-even natural isotopes $_{63}Eu^{151}$ and $_{63}Eu^{153}$. The investigation led to the formulation of decay schemes for $_{62}Sm^{152}$, $_{64}Gd^{152}$ and $_{64}Gd^{154}$. It is the purpose of this section to present those decay schemes together with a discussion of the data leading to them.

Introductory Discussion

Any study of these particular europium isotopes is made difficult by the following fact. A normal sample of europium contains two natural isotopes in nearly equal abundance. Upon irradiation both isotopes give rise to neutron induced activities which (aside from a short isomeric state) have comparable half lives of several years. This situation is further complicated because both beta-minus and K-capture decay processes are known to exist. Thus both Sm and Gd emitters are present in the decay products.

Because of the complexity of the problem of developing decay schemes for the europium isotopes, a number of workers have given time and efforts to attempt a solution. A variety of methods were used in the investigations. The results published to date include:

a. Information obtained from mass-spectrographic techniques by Hayden et al (7)
b. Beta ray spectrographic work of Cork et al (2)
c. Beta-coincidence results of Fowler and Schreffler (3)
d. Assignments from enriched isotopes studies of Katz and Lee (9)
e. Gamma coincidence and beta ray spectrometric work of Slattery et al (14)
f. Studies by Grodzins (5) which classify some of the radiations arising from the nine hour metastable state of Eu^{152}.

The information this author has to contribute comes from three different sources; (a) beta-ray spectrographic data, (b) gamma ray spectrometric results and (c) gamma-gamma coincidence studies.

Beta-ray Spectrographic Data

The data from the first mentioned source resulted from the analysis of 16 photographic plates exposed in beta-ray spectrographs under magnetic field strengths of 222, 382 and 774 gauss. To present a detailed discussion of the instrument and techniques involved is beyond the proposed scope of this thesis. Instead the reader is referred to theses by Mellor (13) and Keshishian (10). The data obtained from the beta-ray spectrograms is presented in its most meaningful form in Table 1.

Column 1 gives the conversion group energies in kilovolts. The following symbols denote those conversion groups which were reported by other workers: [c]Cork, et al (2); [k]Katz and Lee (9); [s]Slattery, et al (14); and [g]Grodzins (5). In addition the symbol, *, identifies those groups which are one or two orders of magnitude more intense than the other groups tabulated.

Column II gives the assumed shell assignments. When conversion groups carry multiple assignments the resulting gamma rays are somewhat questionable.

Column III lists the gamma ray energies for the radiations associated with samarium states.

Column IV lists the gamma ray energies for the radiations associated with gadolinium states.

In Column V the gamma rays are numbered. The letters s,g are used when the data is insufficient to distinguish between samarium and gadolinium. In these cases two gamma rays are reported for the conversion group.

Table 1. Radiations in Sm^{152}, Gd^{152}, and Gd^{154}.

Conversion Energy Kev	Shell	Gamma ray Sm	Energy(Kev) Gd	Gamma ray number
44.5	K	91.3		1
51.3	K	98.1		2
55.3	K	102.1	105.5	3 s,g
64.3	K	111.1		4
70.3	K	117.1	120.5	5 s,g
*72.8[c,k,s,g]	K		123.0	6
*74.6[c,k,s,g]	K	121.4		7
77.0				
79.0	K	125.8	129.2	8 s,g
84.0	L	91. 3		1
89.4	K	136		9
92.0	L	99.2		2
100.4	K	147	151	10 s,g
103.6	L	111.1		4
110.5	K,L		160.7	K 11, L5
* K Series of L's, Ms, Ns, for well known gamma rays 6 & 7				
128.8	K,L	176		K 12, L9
133.5	K	180	184	13 s,g
138.2	K,L	185	188	K 14, L10 s,g
152.5	K		203	15
158.6	K	205	209	16 s,g
164.8	K	212	215	17 s,g
167.9	L	176		12
175.7	K	222	226	18, 19 (perhaps both)
188.7				
194.6	L		202	15
*196.9[c,k,s,g]	K	243.7		20
205.4	K	252	256	21 s,g
213.2	L	222		18
216.2	L		226	19
230.9	K	278		22
*236.7[c]	L	243.9		20
242.3[c]	M	243.7		20
243.9	K,N	290.7		K 23, N20
267.1	K		317	24
275.3	K	322		
277.9	K	325	328	25, 26 (perhaps both)
284.9[c]	K,L		335	K 27, L 23
*293.5[c,k,s,g]	K		343.7	28
302.7				
307.8	L		317	24
316	K,L	363		K 27, L 25
321.5	K,L		372	K 30, L 26
326 [c]	L		334	27
*335.2[c]	L		343	28
341.1[c]	M		343	28

Table 1, Cont'd.

Conversion Energy Kev	Shell	Gamma ray Sm	Energy(Kev) Gd	Gamma ray Number
345.3	K		396	31
350.0	K	395		32
356.7	L	364		29
*359.7[c,s,g]	K		410	33
365.6	L		373	30
377.3	K	424		34
381.8	K		432	35
388.2	K,L		439	K 36, L31,32
395.5	K	443.8		37
400.0	K		450	38
401.6	L		410	33
413.7	K		464	39
418.3	K	465		40
426.6	K,L		476	K 41, L 35
431.5	L		439	36
434.2	K,L		484	K 42, L 37
442	K,L		492	K 43, L 38
451.6	K		502	44
457.5	L	465		39, 40
464.3				
469.3[c]	K,L		520	K 45, L 41
477.2	L		484	42
483.5	L		491	43
494.1	L		502	44
507.8				
514.9	L			45
521.4	K	568		46
531.7	K		582	47
*537.7[c]	K		588	48
545.2	K		595	49
560.6[c]	K,L	608	611	K 50 s,g L 46
574.6	L		582	47
580.9	L		589	48
588.4	L		596	49
591.8				
604.6[c]	L	611	612	50 s,g
622.7	K	670	673	51 s,g
*641.9[c]	K	689		52
654.0	K	700		53
663.3	L	670	671	51 s,g
668.4[c,s]	K	715	719	54 s,g(usually given as 720 Sm)
682.2	L	689		52
691.6	K,L	738	742	K 55,s,g, L 53
703.4	K		753	56
713.7	L	720		54 s(see note on K)
728 [c,s,g]	K		778	57
732.6	L	740	740	55 s,g

Table 1. Cont'd.

Conversion Energy Kev	Shell	Gamma ray Sn	Energy(Kev) Gd	Gamma ray Number
738.4	K		789	58
747.5	K,L		798	K 59, L 56
763.0	K	810	813	60 s,g
771	L		779	57
782.9	K,L	830	833	K 61 s,g L 58
789.4	K,L	836	840	K 62 s,g L 59
796.8	K		847	63
*820.9[c],g	K	867.7	871.1	64 s,g
832.9	K	880	883	65, 66 (perhaps both)
839.5	K,L		889	K 67, L 63
850.6	K		901	68
856	K	903		69
871.9	L	879		65
877.4	L		883	66
885.1	K	932		70
895.4	L	903	903	68, 69
903.4	K		954	71
*916.3[c],s,g	K	963.1		72
923.9	K,L	971	974	K 73 s,g L 70
930	K	977	980	74 s,g
946.6	L		954	71
955.8[c]	L	963		72
965.3	K,L	1012	1015	K 75 s,g L73 s,g
1029.0	K	1076	1079	76 s,g
*1038.6[c],s,g	K	1085.4		77
1055.9	K		1106	78
*1065.2[c],k,s	K	(1112)	1115.4	79 s,g(most likely b)
1077.0	L	1084.2		77
1085.8	K		1136	80
1092.4	K	1139		81
1097.6	K,L	1144	1147	K 82 s,g L 78
1107	L		1115	79 g
1118	K	1165	1168	83 s,g
1130.8	K,L		1181	K 84 L 80,81
1137.6	L	1145	1145	82 s,g
1150.5	K	1197	1200	85 s,g
1161.6	K	1208	1212	86 s,g
1172.0	L		1189	84
1190	K,L	1237	1240	K 87 s,g L85 s,g
1230.8	L	1238	1239	87 s,g
1285.4	K		1336	88
1302.9	K	1350		89
1311.7	K		1362	90
1329.7	K,L	1377	1380	K 91 s,g L87 s,g
1341.9	L	1350		89
1356.7	K,L	1404		K 92 L 90

Table 1. Concl.

Conversion Energy Kev	Shell	Gamma ray Sm	Energy(Kev) Gd	Gamma ray Number
*1362.2[a],g	K	1409	1412.4	93 a,g
1375.4	K	1422	1425	94 a,g
1395.1	K,L	1442	1445	K 95 a,g L 92
1403	K,L	1450	1453	K 96 a,g L 93a,g
1415.8	L	1423	1424	94 a,f
1447.3	K	1494	1498	97 a,g
1462.6	K	1509	1513	98 a,g
1503.5	K,L	1550	1554	K100 a,g L 98a,g
1544.5	K,L	1591	1595	K101 a,g
1554.6	K	1601	1605	K102 a,g
1483	K	1531	1534	K 99 a,g

The general accuracy is such that gamma ray energies reported to tenths of kev are felt to be accurate to within 0.5 kev below energies of 400 kev, and accurate to 1 kev for the remaining gamma rays. Gamma ray energies reported to the nearest kev, may be up to 2 kev in error below energies of 400 kev and up to 4 kev in error for the remaining radiations.

Gamma Ray Spectrum

Plate VI, Curve C is the result of investigations conducted with the scintillation spectrometers described in the section on Instrumentation. The information from this second source does not add much to the general knowledge about the europium isotopes under study. Had there been intense gamma transitions which for some reason were weakly converted in the internal conversion process, the gamma spectrum would have contained peaks marking these transitions at the appropriate energy abscissae. However, no such peaks were revealed on Plate VI. The gamma ray spectrum then served

EXPLANATION OF PLATE VI

Gamma ray spectrum of the neutron induced europium activities.

Operating conditions: High voltage ≐ 940 volts

Window width = 1.0 volts.

————Curve A Original data
- - - - -Curve B Curve A corrected for leakage and background
——·——Curve C Curve B corrected for crystal efficienty

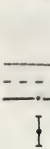

Statistical uncertainties

PLATE VI

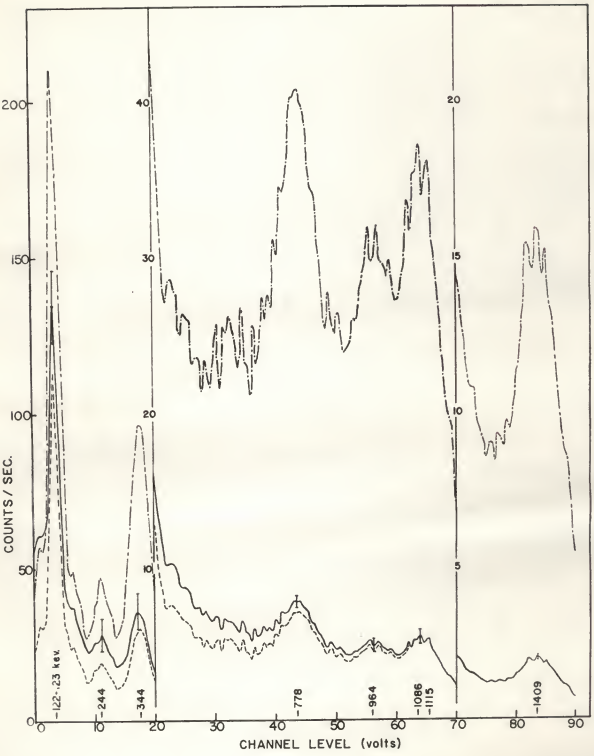
COUNTS / SEC.
CHANNEL LEVEL (volts)
122-123 kev.
244
344
778
964
1086
1115
1409

mainly to emphasize the more intense transitions. These transitions are identified on the plate by energy values (in kev) marked along the energy axis under the more intense peaks.

Coincidence Studies

The third source of information was gamma-gamma coincidence studies carried out with the coincidence spectrometer previously described in the section on Instrumentation. It was here that the scintillation spectrometers were of major use. Plate VII, Curve D, gives the results obtained by adjusting one spectrometer to monitor the 122 Sm - 123 Gd line region while scanning the gamma ray spectrum with the second spectrometer. Plate VIII, Fig. 1 gives similar results for spectrometer one set on the 340 kev region with spectrometer two sweeping the spectrum. Figure 2 of Plate VIII shows two special coincidence studies. In the first, Fig. 2a, spectrometer one was set on the 778 kev transition while the 340 kev region was scanned with instrument two. In the second, Fig. 2b the 200-400 kev region was scanned by spectrometer two while the 1100 kev region was fixed on instrument one.

The following interpretations can be made from Plate VII. The Sm 122 kev transition is in pronounced coincidence with Sm 244 at point (a), Sm 964 at (c), and Sm 1409 at point (e). Somewhat less justified are Sm 122-424 and Sm 122-444 coincidences. The Gd 123 kev line is in coincidence with Gd 1115 at (d) and probably Gd 335 at (b). A possible coincidence exists between Gd 123 and Gd 1453.

Plate VIII, Fig. 1 yields the following information. The Gd 344 transition is coincident with Gd 410 at point (a) and Gd 778 at (b). The rather peculiar line structure of the 344-410 coincidence lines can be explained

EXPLANATION OF PLATE VII

Coincidence spectrum with 122 Sm - 123 Gd kev gamma rays fixed. The letters a,b,d,d,e denote important coincidence peaks.

——·——Uncorrected gamma ray spectrum
————Curve A Original coincidence data
· · · · ·Curve B Curve A partially corrected for mechanical counter losses
- - - - -Curve C Curve B partially corrected for accidental counts
—— ——Curve D Curve A corrected for crystal efficienty

PLATE VII

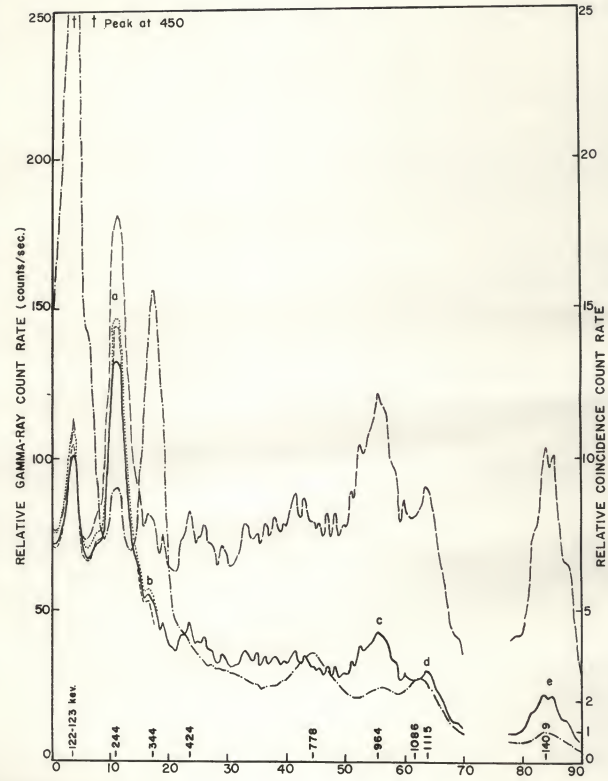
Peak at 450
RELATIVE GAMMA-RAY COUNT RATE (counts/sec.)
RELATIVE COINCIDENCE COUNT RATE
122-123 kev.
244
344
424
778
964
1086
1115
140.9
a
b
c
d
e

EXPLANATION OF PLATE VIII

Fig. 1. Coincidence spectrum with 340 kev region fixed.

Fig. 2a. Coincidence study of 340 kev region with Gd 778 kev fixed.

Fig. 2b. Coincidence study of 200-400 kev region with 1100 kev region fixed.

The letters a,b,c,d,e,f denote important coincidence peaks.

———·———Uncorrected gamma ray spectrum
————————Uncorrected coincidence spectrum

PLATE VIII

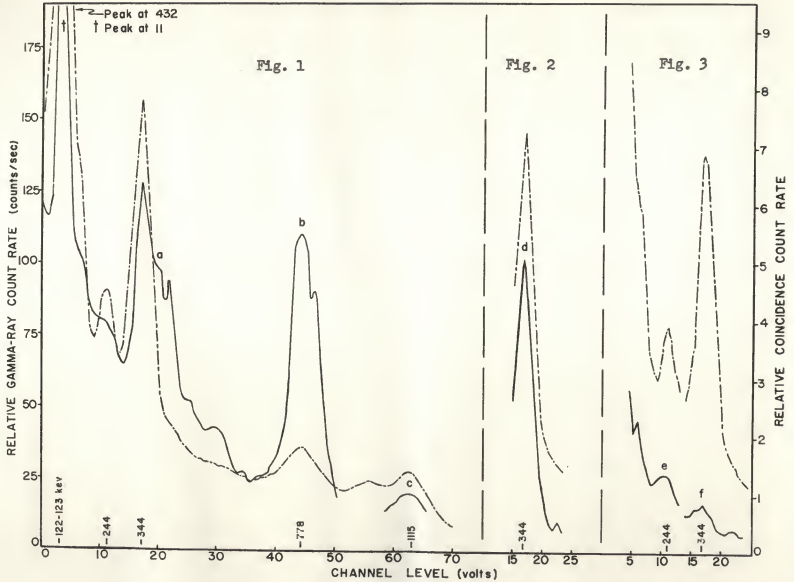
Peak at 432
Peak at 11
Fig. 1
Fig. 2
Fig. 3
RELATIVE GAMMA-RAY COUNT RATE (counts/sec)
RELATIVE COINCIDENCE COUNT RATE
CHANNEL LEVEL (volts)
122-123 kev
244
344
778
1115
a
b
c
d
e
f

upon the basis of admixtures of both lines in each spectrometer. Point (c) of Fig. 1 and point (f) of Fig. 2b announce a Gd 335-1115 coincidence.[1] Figure 2a, point (d) shows that Gd 778 is in coincidence with Gd 344 but not Gd 410. Point (e) represents a possible coincidence between Sm 244 and a weak Sm 1165 transition.

Decay Schemes

The conclusions from the coincidence studies are combined with the other data reported into the decay schemes presented in Plate IX. It is not intended that these schemes be thought of as complete. Rather they are skeleton energy level diagrams. Although no absolute claim to correctness can be made for these decay schemes, they are, nevertheless, consistent with the experimental data reported in this thesis and, in general, with earlier results published by several other investigators (7), (2), (3), (9), (14), (5). The rest of this section will be devoted to a discussion of the particular form of each diagram.

The Sm^{152} decay scheme incorporates the 122-244, 122-964, and 122-1409 kev coincidence results to establish the levels at 366, 1086 and 1531 kev respectively. That the first excited level is 122 kev is well known. Elementary nuclear shell theory supports the 810 kev level. This transition plus appropriate complementary transitions are present in Table 1. Lack of a 122-1086 coincidence points to a 1086 kev transition directly to

---

[1] That the coincidence is 335-1115 and not 344-1115 is argued as follows. Katz and Lee (9) assigned the 344 kev transition to Eu^{152} and the 1115 kev transition to Eu^{154}. Thus the coincidence cannot be 344-1115. However the peak at 344 kev on Plate VI covers up a weaker but well recognized 335 kev gamma ray. Therefore it must be this transition which is in coincidence with the 1115 kev gamma ray.

EXPLANATION OF PLATE IX

Decay scheme of Sm^{152}, Gd^{152} and Gd^{154}. Energy values in kev are given at the left of each level. Transitions observed are shown by arrow-headed lines, with accompanying energy values in kev. A crude measure of the transition intensities is furnished by the heaviness of the transition lines.

PLATE IX

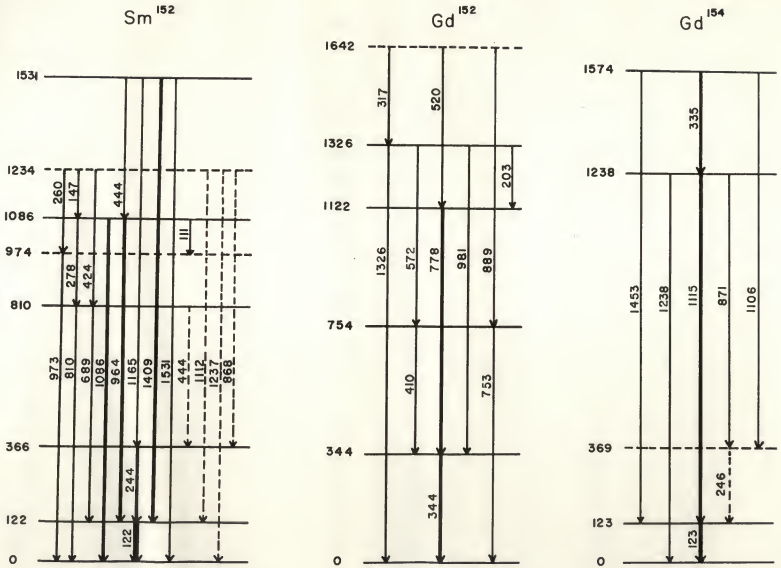
Sm 152
1531
1234
1086
974
810
366
122
0
260
147
444
111
278
424
973
810
689
1086
964
1165
1409
1531
444
1112
1237
968
244
122
Gd 152
1642
1326
1122
754
344
0
317
520
203
1326
572
778
981
889
410
753
344
Gd 154
1574
1238
369
123
0
335
1453
1238
1115
871
1106
246
123

the ground state; hence the 1086 kev level. This last interpretation is contrary to that of Slattery, et al (14). The levels shown dotted were recorded by Grodzins (5) as a result of his studies of a 9-hour metastable state of Eu^{152} which offers an alternate mode of decay to Sm^{152} and Gd^{152}. Some transitions were found to support these levels. However the data collected by this author suggest that the transitions (shown dotted) required to support the 1234 kev level more probably belong to the Gd^{154} decay scheme. If the strong 1112-1115 kev transition belong to Sm^{152}, Grodzins should have observed it. The rest of the transitions shown on the diagram serve to substantiate the levels as established.

The Gd^{152} decay scheme is built around the 344-410 and 344-778 kev coincidences. These together with the lack of a 410-778 kev coincidence establish levels at 754 and 1122 kev. The level at 344 is accepted as the first excited level. Again the 1326 kev level is suggested by Grodzins from his work with the metastable state of Eu^{152}. A number of gamma transitions found in Table 1 are included on the diagram to support these interpretations.

The decay scheme for Gd^{154} embodies the well established first excited level at 123 kev and the 369 kev level recorded by Church and Goldhaber (1) together with the 123-1115 coincidence result. The 1574 kev level is established by the 335-1115 kev coincidence. A weak 123-1453 kev coincidence can be found in Plate VIII to support this last level.

ACKNOWLEDGMENT

The author wishes to express his sincere appreciation to Dr. C. M. Fowler for two fruitful years of instruction, counsel and association. The author is further indebted to the Atomic Energy Commission for their financial support during the past two years.

LITERATURE CITED

1. Church, E. L. and M. Goldhaber.
   Low-Energy Transitions in Gadolinium and Related Rare-Earth Activities. Phys. Rev. 95: 626(A). 1954.

2. Cork, J. M., H. S. Keller, W. C. Rutledge and A. E. Stoddard.
   Additional Electron Lines from Radioactive Europium. Phys. Rev. 77: 848(L). 1952.

3. Fowler, C. M. and R. G. Shreffler.
   The Design of a Magnetic Focusing coincidence Spectrometer. Rev. Sci. Inst. 21: 740. 1950.

4. Green, Alex E. S.
   Nuclear Physics. McGraw-Hill. 1955.

5. Grodzins, I. L.
   Decay of Eu^{152} and Eu^{154}. Amer. Phy. Soc., 1956 Washington Meeting B 10, p. 163.

6. Halliday, D.
   Introductory Nuclear Physics, First Ed. John Wiley and Sons. 1950.

7. Hayden, R. J., M. G. Inghram and J. H. Reynolds.
   Reactions Induced by Slow Neutron Irradiation of Europium. Phys. Rev. 75: Part II 1500. 1949.

8. Instruction Manual, Model 115 Single Channel Pulse Height Analyzer Radiation Instrument Development Laboratory.

9. Katz, R. and M. R. Lee.
   Radioactivity of $Eu^{152, 154}$. Phys. Rev. 85: 1038(L). 1952.

10. Keshishian, V.
    Investigation of the Radioactivity of Terbium 160. Masters Thesis, Department of Physics, Kansas State College, Manhattan, Kansas. 1954.

11. Maeder, D. and V. Wintersteiger.
    Line Shape of Monochromatic Gamma Rays in the Scintillation Spectrometer. Phys. Rev. 87: 537(L). 1952.

12. McGowan, F. K.
    Measure of K-Shell Internal Conversion Coefficients with a Scintillation Spectrometer. Phys. Rev. 93: 163. 1954.

13. Mellor, G. P.
    Design and Construction of a Beta-Ray Spectrometer. Masters Thesis, Department of Physics, Kansas State College, Manhattan, Kansas, 1953.

14. Slattery, R. E., D. C. Lu and M. L. Wiedenbeck.
    Long Lived Radioactivity in Eu^{152} and Eu^{154}. Phys. Rev. 96: 465. 1954.

APPENDIX

Capture Efficiency

The probability that a crystal will capture a given gamma-ray is dependent upon the energy of the gamma-ray. The quantitative measure of this dependence is given by an absorption coefficient.

Let N be the number of gamma-rays that pass thru a thickness r of the crystal. The number of gamma-rays, -dN, that disappear in an additional thickness, dr, of the crystal is proportional to N and to dr.

$$dN = -k\,N\,dr \qquad \text{A-1}$$

where k is the linear absorption coefficient. It is a function of the gamma-ray energy although it is constant for any given energy. For convenience, a mass absorption coefficient u is defined as

$$u = k/d \qquad \text{A-2}$$

where d is the mass density of the crystal. Substituting in (A-1) and integrating gives

$$N = N_o e^{-udr} \qquad \text{A-3}$$

This is the equation which gives the probability that the crystal will capture a gamma-ray having a given energy.

It is necessary to digress at this point to examine the assumption that the absorption coefficient, k, is linear in the sense of equation A-1. This assumption implies that none of the secondary gamma rays resulting from primary Compton scattering are recaptured by the crystal. Experimentally the gamma radiation would have to be collimated into a narrow beam so that all scattering radiation would be lost from the beam.

Such was not the situation in this investigation. Plate X shows the uncorrected gamma ray spectrum resulting from a 662 kev transition in $_{55}Cs^{137}$ as obtained through the use of the scintillation spectrometer described under

EXPLANATION OF PLATE X

Line shape resulting from a 662 kev gamma transition in Cs^{137}

PLATE X


t Peak at 259 t
200
150
100
50
0
COUNTS / SEC.
Cs137
— 183 kev
— ~400
— 662
0
10
20
30
40
CHANNEL LEVEL (volts)

Instrumentation. It can be seen from the contour of the spectrum to the left of the prominent 662 kev peak that a great number of the Compton secondary gamma rays were absorbed by the crystal. Moreover, they were preferentially absorbed as evidenced by the peak occurring at 183 kev and the shoulder around 400 kev. Since there are no gamma transitions in this cesium isotope other than the one at 662 kev, these two peaks are anomolous and are the result of complicated interactions of factors affecting the absorption of gamma radiation.

To treat these interactions analytically leads to quite formidable calculations. At least one general treatment has been presented (11) which takes into account factors like the Klein-Nishina formula.[1] The theoretical curves derived therein bear a resemblance to the one in Plate X thus making it clear that to assume a linear absorption coefficient is not quite realistic. However it was expedient to make the linear assumption. In doing so it was realized that the resultant correction factors were probably too small at high energies by a factor of two or three.

The National Radiac Company who supplied the crystals used in these experiments also supplied the pertinent physical properties of the crystals.[2] The mass density was given as 3.67 gm/cm^3 while the values of μ supplied as a function of gamma ray energy are reproduced in the following table.

Photon Energy	Total Mass Absorption Coefficient, μ	Linear Absorption Coefficient, k
.05mev	10.3 cm^2/gm	37.8 /cm
.1	1.65	6.056
.2	.33	1.211
.5	.094	.345
1.0	.058	.213
2.0	.041	.151

[1] The Klein-Nishina formula in its original form gives the scattering cross section of the primary Compton process as a function of the scattering angle.

[2] National Radiac, Bulletin No.8, "Sintilon Brand Mounted Sodium Iodide (TL) Crystals."

Given equation (A-3) together with the data presented in the table, it remained to derive an expression or expressions which could be used to correct the gamma ray spectrum obtained by using the crystals. What ultimately was desired was a graph giving the capture efficiency vs. gamma-ray energy. The derivation was made difficult because account had to be taken of the shape of the crystal.

What was done was to consider a cylindrically shaped crystal of radius a and height h.[1] The angle which an incoming gamma-ray made with the axis of the crystal was labeled θ. The distance travelled in the crystal by the gamma-ray was denoted by the variable r. The radioactive source emitting the radiation was assumed to be a point source lying exactly on the axis but at a distance z away from the crystal face. The strength of the source was taken to be N_o.

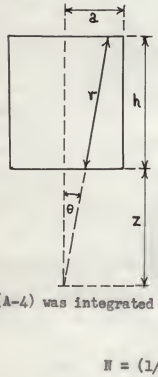

The number of gamma-rays which escaped was expressed as

$$dN = N_o e^{-kr} \frac{d\Omega}{4\pi} \qquad A-4$$

where $d\Omega$ was the solid angle which, in spherical coordinates, was taken as $\sin\theta \, d\theta \, d\phi$.

Equation (A-4) was integrated to give

$$N = (1/4\pi)N_o \int_0^{2\pi} \int_0^{\pi/2} e^{-kr} \sin\theta \, d\theta \, d\phi \, .$$

---

[1] Both crystals used in these experiments had a diameter of 1 3/4 inches and a height of 2 inches.

The ϕ integration was performed leaving

$$N = \tfrac{1}{2}N_o \int_0^{\pi/2} e^{-kr} \sin\theta \, d\theta \qquad \text{A-6}$$

This integral was broken up into three parts. $N = N_1 + N_2 + N_3$

$$N = \tfrac{1}{2}N_o \int_0^{\tan^{-1} a/h+z} e^{-kr} \sin\theta \, d\theta + \tfrac{1}{2}N_o \int_{\tan^{-1} a/h+z}^{\tan^{-1} a/z} e^{-kr} \sin\theta \, d\theta + \tfrac{1}{2}N_o \int_{\tan^{-1} a/z}^{\pi/2} \sin\theta \, d\theta \qquad \text{A-7}$$

In the first integral the variable r was related to the variable θ through the relation $r = h/\cos\theta$. It became convenient to make a change of variable: $x = \cos\theta$. With this change of variable the first integral became

$$N_1 = -\tfrac{1}{2}N_o \int_1^{h+z/R} e^{-kh/x} \, dx \qquad \text{where} \quad R = \sqrt{a^2 + (h+z)^2}$$

A second change of variable with $k\,h/x = w$ reduced the first integral to

$$N_1 = \tfrac{1}{2}khN_o \int_{kh}^{\left[kh/(h+z)\right]R} (e^{-w}/w^2) \, dw$$

An integration by parts resulted in a final expression in which the first term was expressed in closed form in terms of known constants and the second term had the form of the exponential integral function and as such could be evaluated with the aid of specially prepared tables.[1]

$$N_1 = \tfrac{1}{2}khN_o \, e^{-w}/w \Big|_{\left[kh/(h+z)\right]R}^{kh} + \tfrac{1}{2}khN_o \int_{\left[kh/(h+\,z)\right]R}^{kh} (e^{-w}/w) \, dw \qquad \text{A-8}$$

---

[1] Tables of Sines, Cosine and Exponential Ingegrals, Volume II, Federal Works Agency, Work Projects Administration.

The second integral in equation A-7 was considered. From the diagram it was possible to relate r to θ.

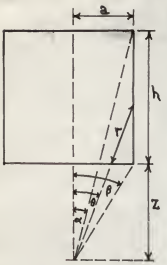

$$r = (a/\sin\theta - z/\cos\theta)$$

Putting this value of r in N_2 gave

$$N_2 = \tfrac{1}{2}N_0 \int_{\tan^{-1} a/h+z}^{\tan^{-1} a/z} e^{-k(a/\sin\theta - z/\cos\theta)} \sin\theta \, d\theta \qquad \text{A-9}$$

This integral could not be evaluated by simple means. However it was integrated numerically by using the trapezoidal rule.

Finally the third integral in (A-7), N_3, was easily integrated and evaluated, the result being

$$N_3 = \tfrac{1}{2}N_0 \cos(\tan^{-1} a/z) \qquad \text{A-10}$$

Combining (A-8), (A-9), and (A-10) and selecting a value of z, it was possible to calculate the number of gamma-rays, N, having any given energy which escaped capture. The efficiency of capture was then (1-N). It was then possible to construct the desired graph of efficiency vs. gamma-ray energy for any given value of z.

At the higher values of z (5-20 cm) the accuracy of the first two integrals began to suffer because of having to difference two nearly equal numbers. To overcome this difficulty the integrals N_1 and N_2 were evaluated by asymptotic expansions. An outline of the derivations in each case is sketched below and the final result recorded.

The expression for the first integral with r replaced by h/cosθ was taken as

$$N_1 = \tfrac{1}{2}N_0 \int_0^{\tan^{-1} a/h+z} e^{-kh/\cos\theta} \sin\theta \, d\theta \qquad \text{A-11}$$

The trigonometric functions were replaced by the first few terms of their series expansion.

$$1/\cos\theta \doteq 1 + \theta^2/2 + \cdots \qquad \sin\theta \doteq \theta - \cdots$$

This gave for (A-11)

$$N_1 \doteq \tfrac{1}{2}N_o \int_0^{\tan^{-1} a/h + z} e^{-kh(1 - \theta^2/2)}\, \theta\, d\theta$$

$$N_1 \doteq N_o e^{-kh}/2kh \left[1 - e^{-\frac{1}{2}kh(\tan^{-1} a/h \;\; z)^2}\right] \qquad \text{A-12}$$

This approximation is accurate to about 1 percent for $z \geq 5$ cm.

The second ingegral, N_2, from A-9 was written as follows

$$N_2 = \tfrac{1}{2}N_o \int_A^B e^{-kr}\, d(\cos\theta) \qquad \text{A-13}$$

The exponential appearing in A-9 was approximated as

$$r = (a/\sin\theta - z/\cos\theta) \doteq a/\sin\theta - z(1 + \tfrac{1}{2}\sin^2\theta + \ldots)$$

To a second order approximation

$$a/\sin\theta \doteq r + z + \tfrac{1}{2}z\sin^2\theta = y + \tfrac{1}{2}z\, a^2/k^2$$

where $\sin\theta = a/r + z$ was taken as the first approximation and $y = r + z$.

Thus $\sin\theta = -d(\cos\theta) \doteq a/(y + \tfrac{1}{2}z\, a^2/y^2) = a/y - \tfrac{1}{2}z\, a^3/y^4 + \cdots$

Also

$$d(\cos\theta) = \frac{\partial(\cos\theta)}{\partial y}\,\frac{\partial y}{\partial r}\, dr = (a^2/y^3)\, dr$$

Putting the appropriate expressions in (A-13) gave

$$N_2 \doteq \tfrac{1}{2}a^2N_o \int_{A'}^{B'} (e^{-kr}/y^3)\, dr \doteq \tfrac{1}{2}a^2N_o e^{kz} \int_{A''}^{B''} (e^{-ky}/y^3)\, dy$$

A change of variable was made by letting $ky = x$. Finally after changing

the limits to allow for all the changes of variables, the resulting expression was

$$N_2 \doteq a^2k^2e^{kz}\int_{k(R' + z)}^{kz} (e^{-x}/x^3)\,dx \qquad \text{where} \quad R' = (h/h + z)\sqrt{a^2 + (h + z)^2}$$

Successive integration by parts resulted in an expression whose first two terms were in closed form while the last term could be evaluated with the aid of a table of exponential integral functions.

$$N_2 \doteq \tfrac{1}{2}a^2k^2N_oe^{kz}\left\{-e^{-x}/2x^2\Big|_{k(R' + z)}^{kz} + \tfrac{1}{2}e^{-x}/x\Big|_{k(R' + z)}^{kz} - \tfrac{1}{2}\int_{k(R^2 + z)}^{kz} e^{-x}/x\,dx\right\} \qquad \text{A-14}$$

The value of N_2 as calculated by (A-14) was estimated to be accurate to within 2 percent for $z \geq 20$cm. It was noted that by virtue of the large values of the exponents involved in the last term, the exponential integral functions themselves could be replaced by their asymptotic expansions.

With the aid of the various formulas given above, graphs of efficiency vs gamma-ray energy were prepared for energies up to two mev and for values of z of 0, .1, 1, 2, 5, and 20 cm. These graphs, shown in Plate XI, were used to make the corrections discussed in the section on Collection and Treatment of Experimental Data.

EXPLANATION OF PLATE XI

Crystal efficiency correction curves.

———Efficiency axis runs from 0-1.0

- - - Efficiency axis runs from 0-0.1

——·—Efficiency axis runs from 0-0.01

PLATE XI

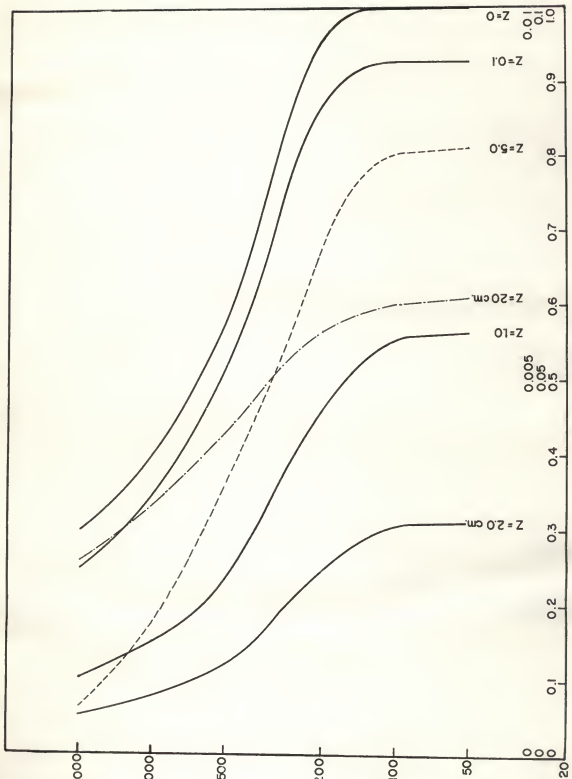
ENERGY (kev.)
2000
1000
500
200
100
50
20
I / EFFICIENCY FACTOR
0.005
0.05
0.1
0.2
0.3
0.4
0.5
0.6
0.7
0.8
0.9
1.0
0.01
0.1
1.0
Z = 2.0 cm.
Z=1.0
Z=20 cm.
Z=5.0
Z=0.1
Z=0

THE APPLICATION OF SCINTILLATION SPECTROSCOPY TO AN INVESTIGATION OF THE NEUTRON INDUCED EUROPIUM ACTIVITIES

by

HAROLD SIMS BUTLER

B. A., Phillips University, 1953

AN ABSTRACT OF A THESIS

submitted in partial fulfillment of the

requirements for the degree

MASTER OF SCIENCE

Department of Physics

KANSAS STATE COLLEGE
OF AGRICULTURE AND APPLIED SCIENCE

1956

An investigation was undertaken of the gamma radiation arising from two neutron induced europium activities, Eu^{152} and Eu^{154}. Two instruments supplied data which greatly facilitated the study--the scintillation spectrometer and the coincidence spectrometer.

The basic operating features of the scintillation spectrometer are discussed. Particular emphasis is placed on the form and reliability of the data recorded by the instrument. The scintillation spectrometer was utilized to obtain the gamma ray spectrum of the decaying activities.

Two scintillation spectrometers were combined with a coincidence counter to form a coincidence spectrometer. This instrument was employed to investigate gamma-gamma coincidences in radiations arising from the isotopes.

Both the gamma ray spectrum and the coincidence spectrum were corrected for factors which tended to reduce their meaningfulness. The gamma ray spectrum was corrected for leakage, background and crystal capture efficiency. The coincidence spectrum was adjusted for losses arising from the dead time of the mechanical ratchet-type counter and for accidental counts and crystal efficiency.

The information taken from the gamma ray spectrum and various coincidence spectra together with accurate transitions energy measurements was utilized to establish decay schemes for Sm^{152}, Gd^{152} and Gd^{154}. Transition energies were calculated from beta ray spectrographic analysis of the internal conversion spectrum. The decay schemes presented are consistent with the results of this investigation and, in general, with conclusions reported earlier by other workers.